AIMS Mathematics, 11(3): 5911–5935.
DOI: 10.3934/math.2026244
Received: 13 November 2025
Revised: 03 February 2026
Accepted: 02 March 2026
Published: 09 March 2026

https://www.aimspress.com/journal/Math

Research article

Fractional-order multi-parametric methods for nonlinear problems

Ahmad Alalyani*

Department of Mathematics, Faculty of Science, Al-Baha University, Al-Baha 65526, Saudi Arabia

* **Correspondence:** Email: azaher@bu.edu.sa.

Abstract: In this research, a two-step bi- and tri-parametric iterative method is developed for solving nonlinear equations employing the Caputo fractional derivative. The theoretical convergence analysis demonstrates that the proposed schemes achieve an order of convergence of $2\tau+1$, where τ denotes the order of the Caputo fractional operator. In addition, fractal analysis is employed to identify effective initial values that enhance numerical performance. To compare the suggested scheme's efficacy and stability to existing approaches, several nonlinear engineering problems are examined. The numerical results demonstrate that, compared with existing methods, the proposed schemes achieve lower residual errors, higher convergence rates, reduced memory consumption, improved error profiles, and superior computational orders of convergence, thereby making them a more efficient and reliable alternative for solving problems in science and engineering.

Keywords: fractional order scheme; convergence analysis; stability analysis; dynamical planes; biomedical engineering applications
Mathematics Subject Classification: 65H04, 65H05, 65B99, 65Y15, 65Y04

1. Introduction

Nonlinear equations are the foundation of many natural and engineering problems that arise in mathematical modeling. They reflect the nonlinear behavior of systems and have been studied for many decades, particularly when the variables' interactions are complex or fail linear proportionality. Nonlinear equations of the form

$$g(x) = 0 \tag{1.1}$$

are utilized across numerous scientific and engineering areas, including physics, biology, engineering, and biomedicine. Some of the most significant applications include nonlinear vibrations, fluid dynamics, population dynamics, and brain function, among others. The intrinsic nonlinearity of these systems can lead to multiple real or complex solutions, sensitivity to initial conditions, and typically result in iterative nonconvergent behavior, all of which restrict the application of traditional

analytical methods [1–3]. Due to these limitations, the majority of researchers in applied mathematics and computer science employ iterative and numerical techniques to provide approximate solutions to nonlinear problems with a reasonable level of accuracy and precision. In addition to facilitating computational practice, these methods offer deeper insights through stability, convergence, and dynamic analysis of nonlinear problems in science and engineering [4]. However, despite their advantages, traditional numerical approaches have limitations such as instability, divergence, and precision loss. To increase accuracy, robustness, and reliability when handling highly nonlinear systems, fractional-order, hybrid, and intelligent techniques have been investigated [5]. To obtain analytical solutions to nonlinear problems, analytical or semi-analytical techniques are employed [6]. These methods produce exact or closed-form solutions that describe the problem's nonlinear behavior while providing valuable theoretical insights into the dynamics of nonlinear phenomena [7–9]. However, they are not appropriate for complex or high-dimensional nonlinear problems [10], as their solutions are restricted to specific functional representations or simplified assumptions. Nonlinear equations of higher degree or fractional order must be solved efficiently using numerical schemes because they are solutions iteratively using some initial approximations close to the exact solution of the problem [11–13]. Although iterative approaches can be effective, there are certain limitations:

- Iterative techniques rely heavily on accurate initial estimates and may fail to converge, or may converge to undesirable roots in the presence of multiple roots, due to their local convergence nature.
- Certain classical techniques become computationally expensive and require a significant amount of processing time and memory when applied to large-scale systems or high-accuracy problems.
- The iterative map becomes unstable when the function's derivative is close to zero, which frequently leads to divergence.
- Such approaches are frequently inconsistent and are susceptible to round-off errors at discontinuities or singularities in the problem.

Fractional-order schemes [14–16] have become a practical and flexible alternative for the modeling and solution of fractional-order nonlinear equations and their systems, helping to overcome the limitations of traditional numerical approaches. This is particularly significant when concepts such as memory effects, hereditary behavior, and unusual dispersion cannot be well explained by normal integer-order models [17–19]. Fractional-order derivatives usually expressed by operators such as those of Caputo, Grünwald–Letnikov [20], or Riemann–Liouville [21], replace normal integer-order derivatives in these sophisticated formulations. High-accuracy discretization for time-diffusion-type nonlinear problems has been advanced in [22–24] via precise interpolation and compact finite difference schemes, while efficient time integration has been achieved through variable stepsize block methods and optimized A-stable hyperbolic fitting techniques [25, 26]. Although they naturally encompass nonlocal and history-dependent phenomena, fractional-order iterative schemes provide a more thorough and accurate representation of issue behavior in physical, biological, and engineering models. In contrast to classical iterative techniques, which only address immediate and local interactions, fractional structures have long-range interdependence from the very beginning of the process.

They enhance numerical computation's flexibility, stability, consistency, accuracy, precision, and convergence behavior, resulting in physically consistent and resilient solutions to nonlinear equations [27]. Fractional-order formulations can address the limitations of standard iterative

approaches, such as sensitivity to starting guess values and divergence in stiff or ill-conditioned systems, by introducing additional complexity [28, 29]. This enhanced flexibility allows for more precise control over computational efficiency and solution accuracy, making fractional approaches appropriate for highly nonlinear or multiscale situations in which traditional methods exhibit low convergence rates and reduce the order of convergence.

Motivated by the limitations in classical iterative techniques and recent developments in fractional sceheme, the main aim and novel contributions of this investigation are characterized as follows:

- The development of bi- and tri-parametric families of two-step fractional-order iterative methods for solving nonlinear equations.
- The suggested fractional-order schemes' local convergence analysis will be computed using a generalized Taylor series expansion in a Caputo-type framework.
- Zones of attraction are generated to investigate the stability and dynamical features of the fractional iterative systems under various initial conditions.
- Visualize convergence points, and then compute percentage convergence and dynamical planes to evaluate the overall performance and reliability of the approaches under consideration.
- The effectiveness of the fractional algorithms designed to solve nonlinear models is evaluated using a set of numerical test problems. The results are examined in terms of CPU time, computational order of convergence (COC), residual error, and graphical representations.

Furthermore, the proposed bi- and tri-parametric fractional iterative families add flexibility by allowing fine-tuning of the parameter between computational cost and solution precision through fractional parameter adjustment, as well as a best alternative to compute efficient solution solvers for nonlinear engineering problems.

The paper is organized as follows. Section 2 presents the theoretical background, preliminary concepts, and additional details regarding the proposed fractional-order iterative algorithms. Section 3 describes the numerical implementation and evaluation criteria, including comparisons with existing approaches, implementation procedures, computer specifications, and pseudocode representations of the algorithms. Section 4 provides numerical experiments and engineering test problems that demonstrate the effectiveness of the proposed methods. Section 5 highlights the main results and limitations, and proposes directions for future research.

2. Development and analysis of the fractional scheme

This section discusses the theoretical basis and derivation of the proposed fractional iterative techniques for solving nonlinear equations involving Caputo-type fractional derivatives. The Caputo fractional derivative is adopted due to its consistency with classical differential operators and standard initial conditions. In particular, the Caputo derivative assigns a zero derivative to constant functions, thereby preserving a key property of classical calculus; this behavior is generally not shared by the Atangana–Baleanu or Caputo–Fabrizio operators. This property enables a direct extension of the proposed iterative scheme and convergence analysis to nonlinear equations without altering the underlying theoretical structure. First, the fundamental definitions, properties, and applications of fractional calculus in science and engineering, which serve as the analytical foundation for the proposed method, are reviewed. The local theoretical convergence analysis is presented at the end of this section.

2.1. Preliminaries

Definition 1. *The gamma function [30], also known as the generalized factorial function, is defined as follows:*

$$\Gamma(x) = \int_0^{+\infty} u^{x-1} e^{-u}\, du, \tag{2.1}$$

where $x > 0$, with $\Gamma(1) = 1$ and $\Gamma(n+1) = n!$ for $n \in \mathbb{N}$.

Definition 2. *Let*

$$g : \mathbb{R} \to \mathbb{R}, \quad g \in \mathbb{C}^{+\infty}([\tau, x]),\ -\infty < \tau < x < +\infty,\ \tau \geq 0,\ m = \lfloor \tau \rfloor + 1. \tag{2.2}$$

The Caputo fractional derivative [31] of order τ is defined as follows:

$$\left[{}_C\partial_{\tau_1}^{\tau}\right] g(x) = \begin{cases} \dfrac{1}{\Gamma(m-\tau)} \displaystyle\int_0^x \frac{d^m}{dt^m} g(t) \frac{1}{(x-t)^{\tau-m+1}}\, dt, & \tau \notin \mathbb{N}, \\ \dfrac{d^{m-1}}{dt^{m-1}} g(x), & \tau = m-1 \in \mathbb{N} \cup \{0\}, \end{cases} \tag{2.3}$$

where $\Gamma(x)$ is the gamma function.

2.2. Fractional Taylor expansion

Theorem 3. *(Generalized Taylor formula [32,33]) Suppose $\left[{}_C\partial_{\tau_1}^{\gamma\tau}\right] g(x) \in \check{c}([\tau_1, \tau_2])$ for $\gamma = 1, \ldots, n+1$ and $\tau \in (0, 1]$. Then,*

$$g(x) = \sum_{i=0}^{n} \left[{}_C\partial_{\tau_1}^{i\tau}\right] g(\tau_1) \frac{(x-\tau_1)^{i\tau}}{\Gamma(i\tau+1)} + \left[{}_C\partial_{\tau_1}^{(n+1)\tau}\right] g(\xi) \frac{(x-\tau_1)^{(n+1)\tau}}{\Gamma((n+1)\tau+1)}, \tag{2.4}$$

where $\tau_1 \leq \xi \leq x$, $\forall x \in (\tau_1, \tau_2]$. Higher-order Caputo derivatives are recursively defined as follows:

$$\left[{}_C\partial_{\tau_1}^{n\tau}\right] = \underbrace{\left[{}_C\partial_{\tau_1}^{\tau}\right]\left[{}_C\partial_{\tau_1}^{\tau}\right] \cdots \left[{}_C\partial_{\tau_1}^{\tau}\right]}_{n\text{-times}}. \tag{2.5}$$

Expanding $g(x)$ about ξ gives

$$g(x) = \frac{\left[{}_C\partial_{\xi}^{\tau}\right] g(\xi)}{\Gamma(\tau+1)} (x-\xi)^{\tau} + \frac{\left[{}_C\partial_{\xi}^{2\tau}\right] g(\xi)}{\Gamma(2\tau+1)} (x-\xi)^{2\tau} + O\Big((x-\xi)^{3\tau}\Big). \tag{2.6}$$

Factoring the leading term gives

$$g(x) = \frac{\left[{}_C\partial_{\xi}^{\tau}\right] g(\xi)}{\Gamma(\tau+1)} \left[(x-\xi)^{\tau} + \check{c}_2 (x-\xi)^{2\tau}\right] + O\Big((x-\xi)^{3\tau}\Big), \tag{2.7}$$

where

$$h_j = \frac{\Gamma(\tau+1)}{\Gamma(j\tau+1)} \frac{{}_C\partial_{\tau_1}^{j\tau} g(\xi)}{{}_C\partial_{\tau_1}^{\tau} g(\xi)}, \quad j \geq 2. \tag{2.8}$$

The corresponding fractional derivative is

$$\left[{}_C\partial_{\xi}^{\tau}\right] g(x) = \frac{\left[{}_C\partial_{\xi}^{\tau}\right] g(\xi)}{\Gamma(\tau+1)} \left[\Gamma(\tau+1) + \frac{\Gamma(2\tau+1)}{\Gamma(\tau+1)} \check{c}_2 (x-\xi)^{\tau}\right] + O\Big((x-\xi)^{2\tau}\Big). \tag{2.9}$$

2.3. Existing fractional iterative schemes

The general family of single-step fractional schemes, denoted by SNF_*, is given by

$$x_{i+1} = x_i - \left[\Gamma(\tau+1)\frac{g(x_i)}{{}_C\partial^{\tau}_{\tau_1} g(x_i)}\right]^{1/\tau}, \tag{2.10}$$

with the error relation

$$e^*_{i+1} = \frac{\Gamma(2\tau+1) - \Gamma^2(\tau+1)}{\tau\Gamma^2(\tau+1)} h_2 e_i^{\tau+1} + O(e_i^{2\tau+1}). \tag{2.11}$$

Shams et al. [35] proposed a modified single-step scheme

$$x_{i+1} = x_i - \left[\Gamma(\tau+1)\frac{g(x_i)}{{}_C\partial^{\tau}_{\tau_1} g(x_i)}\frac{1}{1-\beta\frac{g(x_i)}{1+g(x_i)}}\right]^{1/\tau}, \tag{2.12}$$

satisfying

$$e^*_{i+1} = \frac{\Gamma(2\tau+1) - \Gamma^2(\tau+1)}{\tau\Gamma^2(\tau+1)} h_2 e_i^{\tau+1} + O(e_i^{2\tau+1}). \tag{2.13}$$

Similarly, an improved two-stage variant is presented in [34] (abbreviated as GCM) and defined as follows:

$$\begin{cases} y_i = x_i - \left[\Gamma(\tau+1)\frac{g(x_i)}{{}_C\partial^{\tau}_{\tau_1} g(x_i)}\right]^{1/\tau}, \\ x_{i+1} = y_i - \left[\Gamma(\tau+1)\frac{g(y_i)}{{}_C\partial^{\tau}_{\tau_1} g(x_i)}\right]^{1/\tau}, \end{cases} \tag{2.14}$$

with the corresponding error

$$e^*_{i+1} = \frac{-\Gamma(2\tau+1) - \Gamma^2(\tau+1)}{\tau^2\Gamma^2(\tau+1)} + O(e_i^{\tau^2+2\tau+1}). \tag{2.15}$$

Shams et al. [35] further proposed a two-step fractional method (abbreviated as SHM)

$$\begin{cases} y_i = x_i - \left[\Gamma(\tau+1)\frac{g(x_i)}{{}_C\partial^{\tau}_{\tau_1} g(x_i)}\right]^{1/\tau}, \\ x_{i+1} = y_i - \left[\Gamma(\tau+1)\frac{g(y_i)}{{}_C\partial^{\tau}_{\tau_1} g(x_i)}\left(1 + \frac{\frac{g(y_i)}{g(x_i)}}{1-\beta\left(\frac{g(y_i)}{g(x_i)}\right)^2}\right)\right]^{1/\tau}, \end{cases} \tag{2.16}$$

with the error

$$e^*_{i+1} = \left[\frac{(2^{\tau})^2\Gamma(\tau+\frac{1}{2})h_2^2}{\tau\Gamma(\tau)\sqrt{\pi}} - h_2^2\right] e_i^{2\tau+1} + O(e_i^{3\tau+1}). \tag{2.17}$$

Nasir et al. [36] developed another two-step scheme (abbreviated as NAM)

$$\begin{cases} y_i = x_i - \Gamma(\tau+1)\frac{g(x_i)}{{}_C\partial^{\tau}_{\tau_1} g(x_i) - \beta g(x_i)}, \\ x_{i+1} = y_i - \Gamma(\tau+1)\frac{g(y_i)}{{}_C\partial^{\tau}_{\tau_1} g(x_i) - \beta g(y_i)}, \end{cases} \tag{2.18}$$

satisfying

$$e^*_{i+1} = \frac{h_2^{\tau}}{\tau\Gamma(\tau+1)} e_i^{2\tau^2} + \frac{\left(\frac{\beta}{\Gamma(\tau+1)}\right)^{\tau}}{\Gamma(\tau+1)} + O(e_i^{3\tau^2}). \tag{2.19}$$

2.4. Proposed fractional schemes

Motivated by the above formulations, we introduce new bi- and tri-parametric fractional schemes for solving nonlinear equations.

Bi-parametric fractional scheme ($\mathbf{MAB_1}$):

$$\begin{cases} y_i = x_i - \left[\Gamma(\tau+1)\frac{g(x_i)}{{}_C\partial^{\tau}_{\tau_1} g(x_i) - \beta_0 g(x_i)}\right]^{1/\tau}, \\ x_{i+1} = y_i - \Gamma(\tau+1)\left(\frac{g(y_i)}{{}_C\partial^{\tau}_{\tau_1} g(x_i)} + \beta_1\left(\frac{g(y_i)}{{}_C\partial^{\tau}_{\tau_1} g(x_i)}\right)^3\right), \end{cases} \tag{2.20}$$

where $\beta_0, \beta_1 \in \mathbb{R}$.

Tri-parametric fractional scheme ($\mathbf{MAB_2}$):

$$\begin{cases} y_i = x_i - \left[\Gamma(\tau+1)\frac{g(x_i)}{{}_C\partial^{\tau}_{\tau_1} g(x_i) - \beta_0 g(x_i)}\right]^{1/\tau}, \\ x_{i+1} = y_i - \Gamma(\tau+1)\left(\frac{g(y_i)}{{}_C\partial^{\tau}_{\tau_1} g(x_i)} + \beta_1\left(\frac{g(y_i)}{{}_C\partial^{\tau}_{\tau_1} g(x_i)}\right)^3 + \beta_2\left(\frac{g(y_i)}{{}_C\partial^{\tau}_{\tau_1} g(x_i)}\right)^4\right), \end{cases} \tag{2.21}$$

where $\beta_2 \in \mathbb{R}$.

Remark 4. *The tri-parametric fractional scheme MAB_2 given in* (2.21) *can be naturally extended to an n-parametric family by introducing higher-order correction terms into the update formula. In particular, the second step can be written in the following general form:*

$$x_{i+1} = y_i - \Gamma(\tau+1)\sum_{k=1}^{n}\beta_k\left(\frac{g(y_i)}{{}_C\partial^{\tau}_{\tau_1} g(x_i)}\right)^k, \tag{2.22}$$

where $\beta_k \in \mathbb{R}$ for $k = 1, 2, \ldots, n$. This extension preserves the convergence order under the same consistency conditions on β_k. However, larger values of n increase the computational cost due to additional nonlinear evaluations; therefore, a moderate choice of n provides a suitable balance between flexibility and efficiency.

2.4.1. Local convergence

The local convergence behavior of the proposed fractional schemes is established in Theorem 5 using the fractional Taylor expansion.

Theorem 5. *Let $g : \mathbb{R}^n \to \mathbb{R}^n$ be continuously differentiable in a neighborhood of the root ζ. If the initial guess x_0 is sufficiently close to ζ, then the proposed fractional two-step iterative scheme (2.20) attains an optimal convergence order of* $(2\tau+1)$. *The corresponding error relation is expressed as follows:*

$$e^*_{i+1} = \left[\frac{h_2^2(2^{\tau})^4}{\pi\tau^2\Gamma^2(\tau)\Gamma^2\left(\tau+\frac{1}{2}\right)} - \frac{h_2^2(2^{\tau})^2}{\sqrt{\pi}\tau\Gamma(\tau)}\Gamma\left(\tau+\tfrac{1}{2}\right) - \frac{\beta_0 h_2(2^{\tau})^2}{\sqrt{\pi}\tau^2\Gamma^2(\tau)}\Gamma\left(\tau+\tfrac{1}{2}\right)\right]e_i^{2\tau+1} + O\left(e_i^{3\tau+1}\right), \tag{2.23}$$

where

$$h_j = \frac{\Gamma(\tau+1)}{\Gamma(j\tau+1)} \frac{{}_C\partial^{j\tau}_{\tau_1} g(\xi)}{{}_C\partial^{\tau}_{\tau_1} g(\xi)}, \quad j \geq 2.$$

Proof. Let $e^*_{i+1} = x_{i+1} - \xi$ and $e_i = x_i - \xi$ denote the errors in x_{i+1} and x_i, respectively. Expanding $g(x_i)$ around ξ using the generalized Taylor formula gives

$$g(x_i) = \frac{{}_C\partial^{\tau}_{\tau_1} g(\xi)}{\Gamma(\tau+1)} \left[e_i + h_2 e_i^2 + h_3 e_i^3 + h_4 e_i^4 + \cdots \right]. \tag{2.24}$$

Taking the fractional derivative of (2.24), we obtain

$${}_C\partial^{\tau}_{\tau_1} g(x_i) = \frac{{}_C\partial^{\tau}_{\tau_1} g(\xi)}{\Gamma(\tau+1)} \left[\Gamma(\tau+1) + \frac{\Gamma(2\tau+1) h_2 e_i^{\tau}}{\Gamma(\tau+1)} + \frac{\Gamma(3\tau+1) h_3 e_i^{2\tau}}{\Gamma(2\tau+1)} + \cdots \right]. \tag{2.25}$$

Taking the inverse of (2.25) yields

$$\begin{aligned} \frac{1}{{}_C\partial^{\tau}_{\tau_1} g(x_i)} = {} & \frac{1}{\Gamma(\tau+1)} - \frac{\Gamma(2\tau+1) h_2 e_i^{\tau}}{(\Gamma(\tau+1))^3} \\ & + \frac{e_i^{2\tau}}{\Gamma(\tau+1)} \left[-\frac{\Gamma(3\tau+1) h_3}{\Gamma(\tau+1)\Gamma(2\tau+1)} + \frac{(\Gamma(2\tau+1))^2 h_2^2}{(\Gamma(\tau+1))^4} \right] \\ & + \frac{e_i^{3\tau}}{\Gamma(\tau+1)} \left[\frac{h_2 \Gamma(3\tau+1) h_3}{(\Gamma(\tau+1))^3} - \frac{((\Gamma(2\tau+1))^3 h_2^2 - \Gamma(3\tau+1) h_3 (\Gamma(\tau+1))^3) h_2}{(\Gamma(\tau+1))^6} \right]. \end{aligned} \tag{2.26}$$

The error in ${}_C\partial^{\tau}_{\tau_1} g(x_i) - \beta_0 g(x_i)$ in the first substep of the MAB_1 method is

$$\begin{aligned} {}_C\partial^{\tau}_{\tau_1} g(x_i) - \beta_0 g(x_i) = {} & \Gamma(\tau)\tau + \left(-\beta_0 + \frac{(2^{\tau})^2 h_2}{\sqrt{\pi}} \Gamma\left(\tau + \tfrac{1}{2}\right) \right) e_i^{\tau} \\ & + \left(-\beta_0 h_2 + \frac{h_3 (3^{\tau})^3 \sqrt{3}}{2\sqrt{\pi}(2^{\tau})^2} \Gamma\left(\tau + \tfrac{1}{3}\right) \Gamma\left(\tau + \tfrac{2}{3}\right) (\Gamma(\tau + 1/2))^{-1} \right) e_i^{2\tau} \\ & - \beta_0 h_3 e_i^3 - \beta_0 h_4 e_i^4 + O(e_i^5). \end{aligned} \tag{2.27}$$

Taking the inverse of (2.27) yields

$$\frac{1}{{}_C\partial^{\tau}_{\tau_1} g(x_i) - \beta_0 g(x_i)} = \frac{1}{\Gamma(\tau)\tau} - \frac{e_i^{\tau}}{(\Gamma(\tau))^2 \tau^2} \left[-\beta_0 + \frac{(2^{\tau})^2 h_2}{\sqrt{\pi}} \Gamma\left(\tau + \tfrac{1}{2}\right) \right] + O(e_i^{2\tau}). \tag{2.28}$$

Substituting these results into the fractional correction expression

$$\frac{g(x_i)}{g'(x_i) - \beta_0 g(x_i)} = \frac{e_i}{\Gamma(\tau)\tau} + \left(\frac{h_2}{\Gamma(\tau)\tau} + \frac{\beta_0}{(\Gamma(\tau))^2 \tau^2} - \frac{(2^{\tau})^2 h_2 \Gamma(\tau + \frac{1}{2})}{(\Gamma(\tau))^2 \tau^2 \sqrt{\pi}} \right) e_i^2 + O(e_i^3), \tag{2.29}$$

we compute the first-step error as

$$y_i - \xi = \left(-h_2 - \frac{\beta_0}{\Gamma(\tau)\tau} + \frac{(2^{\tau})^2 h_2}{\Gamma(\tau)\tau\sqrt{\pi}} \Gamma\left(\tau + \tfrac{1}{2}\right) \right) e_i^{\tau+1}$$

$$+\left[\frac{h_3(3^\tau)^3\sqrt{3}}{2\Gamma(\tau)\tau\sqrt{\pi}(2^\tau)^2}\Gamma\left(\tau+\tfrac{1}{3}\right)\Gamma\left(\tau+\tfrac{2}{3}\right)(\Gamma(\tau+1/2))^{-1}-h_3-\frac{\beta_0^2}{(\Gamma(\tau))^2\tau^2}+2\frac{\beta_0h_2(2^\tau)^2\Gamma(\tau+1/2)}{(\Gamma(\tau))^2\tau^2\sqrt{\pi}}+\right.$$
$$\left.\frac{(2^\tau)^2h_2^2\Gamma(\tau+1/2)}{\Gamma(\tau)\tau\sqrt{\pi}}-\frac{(2^\tau)^4h_2^2(\Gamma(\tau+1/2))^2}{(\Gamma(\tau))^2\tau^2\pi}-2\frac{\beta_0h_2}{\Gamma(\tau)\tau}\right]e_i^{2\tau+1}+O(e_i^{3\tau+1}). \tag{2.30}$$

Expanding $g(y_i)$ around ξ and simplifying gives

$$\frac{g(y_i)}{{}_C\partial_{\tau_1}^\tau g(x_i)}=\left(-\frac{h_2}{\Gamma(\tau)\tau}-\frac{\beta_0}{(\Gamma(\tau))^2\tau^2}+\frac{(2^\tau)^2h_2\Gamma(\tau+1/2)}{(\Gamma(\tau))^2\tau^2\sqrt{\pi}}\right)e_i^{\tau+1}$$
$$+\left(3\frac{\beta_0h_2(2^\tau)^2\Gamma(\tau+1/2)}{(\Gamma(\tau))^3\tau^3\sqrt{\pi}}+\frac{h_3(3^\tau)^3\sqrt{3}}{2(\Gamma(\tau))^2\tau^2\sqrt{\pi}(2^\tau)^2}-\frac{h_3}{\Gamma(\tau)\tau}-\frac{\beta_0^2}{(\Gamma(\tau))^3\tau^3}+\right.$$
$$\left.2\frac{(2^\tau)^2\Gamma(\tau+1/2)h_2^2}{(\Gamma(\tau))^2\tau^2\sqrt{\pi}}-2\frac{(2^\tau)^4(\Gamma(\tau+1/2))^2h_2^2}{(\Gamma(\tau))^3\tau^3\pi}-2\frac{\beta_0h_2}{(\Gamma(\tau))^2\tau^2}\right)e_i^{2\tau+1}+O(e_i^{3\tau+1}). \tag{2.31}$$

$$\left(\frac{g(y_i)}{{}_C\partial_{\tau_1}^\tau g(x_i)}\right)^3=\left(C_6\right)e_i^{5\tau+1}+\left(C_7\right)e_i^{6\tau+1}+O(e_i^{7\tau+1}), \tag{2.32}$$

where

$$C_6=\frac{\beta_0h_2^3(2^\alpha)^6}{\pi^{3/2}\alpha^6(\Gamma(\alpha))^6}\left(\Gamma\left(\alpha+\tfrac{1}{2}\right)\right)^3-3\frac{\beta_0h_2^3(2^\alpha)^4}{\pi\alpha^5(\Gamma(\alpha))^5}\left(\Gamma\left(\alpha+\tfrac{1}{2}\right)\right)^2+3\frac{\beta_0h_2^3(2^\alpha)^2}{\sqrt{\pi}\alpha^4(\Gamma(\alpha))^4}\Gamma\left(\alpha+\tfrac{1}{2}\right)-\frac{\beta_0h_2^3}{\alpha^3(\Gamma(\alpha))^3}$$
$$-3\frac{\beta\beta_0h_2^2(2^\alpha)^4}{\pi\alpha^6(\Gamma(\alpha))^6}\left(\Gamma\left(\alpha+\tfrac{1}{2}\right)\right)^2+6\frac{\beta\beta_0h_2^2(2^\alpha)^2}{\sqrt{\pi}\alpha^5(\Gamma(\alpha))^5}\Gamma\left(\alpha+\tfrac{1}{2}\right)-3\frac{\beta\beta_0h_2^2}{\alpha^4(\Gamma(\alpha))^4}+3\frac{\beta^2\beta_0h_2(2^\alpha)^2}{\sqrt{\pi}\alpha^6(\Gamma(\alpha))^6}\Gamma\left(\alpha+\tfrac{1}{2}\right)$$
$$-3\frac{\beta^2\beta_0h_2}{\alpha^5(\Gamma(\alpha))^5}-\frac{\beta^3\beta_0}{\alpha^6(\Gamma(\alpha))^6}$$

and

$$C_7=6\frac{\beta_0h_2^2h_3(2^\alpha)^2}{\sqrt{\pi}\alpha^4(\Gamma(\alpha))^4}\Gamma\left(\alpha+\tfrac{1}{2}\right)+33\frac{\beta\beta_0h_2^3(2^\alpha)^2}{\sqrt{\pi}\alpha^5(\Gamma(\alpha))^5}\Gamma\left(\alpha+\tfrac{1}{2}\right)+42\frac{\beta^2\beta_0h_2^2(2^\alpha)^2}{\sqrt{\pi}\alpha^6(\Gamma(\alpha))^6}\Gamma\left(\alpha+\tfrac{1}{2}\right)$$
$$+15\frac{\beta^3\beta_0h_2(2^\alpha)^2}{\sqrt{\pi}\alpha^7(\Gamma(\alpha))^7}\Gamma\left(\alpha+\tfrac{1}{2}\right)-3\frac{\beta_0h_2^2h_3}{\alpha^3(\Gamma(\alpha))^3}-6\frac{\beta\beta_0h_2^3}{\alpha^4(\Gamma(\alpha))^4}-15\frac{\beta^2\beta_0h_2^2}{\alpha^5(\Gamma(\alpha))^5}-12\frac{\beta^3\beta_0h_2}{\alpha^6(\Gamma(\alpha))^6}-3\frac{\beta^4\beta_0}{\alpha^7(\Gamma(\alpha))^7}.$$

By including the parameter β_1 in the second substep of the MAB_1 scheme and adding (2.30) and (2.32), we obtain

$$B_1^{[*]}=\left(\frac{g(y_i)}{{}_C\partial_{\tau_1}^\tau g(x_i)}\right)+\beta_1\left(\frac{g(y_i)}{{}_C\partial_{\tau_1}^\tau g(x_i)}\right)^3, \tag{2.33}$$

and substituting

$$B_1^{[*]}=\left(-\frac{h_2}{\Gamma(\tau)\tau}-\frac{\beta_0}{(\Gamma(\tau))^2\tau^2}+\frac{(2^\tau)^2h_2}{(\Gamma(\tau))^2\tau^2\sqrt{\pi}}\Gamma\left(\tau+\tfrac{1}{2}\right)\right)e_i^{\tau+1}$$
$$+\left(3\frac{\beta_0h_2(2^\tau)^2\Gamma\left(\tau+\frac{1}{2}\right)}{(\Gamma(\tau))^3\tau^3\sqrt{\pi}}+\frac{h_3(3^\tau)^3\sqrt{3}}{2(\Gamma(\tau))^2\tau^2\sqrt{\pi}(2^\tau)^2}-\frac{h_3}{\Gamma(\tau)\tau}-\frac{\beta_0^2}{(\Gamma(\tau))^3\tau^3}\right)e_i^{2\tau+1}$$

$$+\left(2\frac{(2^{\tau})^2\Gamma\left(\tau+\frac{1}{2}\right)h_2^2}{(\Gamma(\tau))^2\tau^2\sqrt{\pi}}-2\frac{(2^{\tau})^4(\Gamma(\tau+\frac{1}{2}))^2h_2^2}{\pi(\Gamma(\tau))^3\tau^3}-2\frac{\beta_0h_2}{(\Gamma(\tau))^2\tau^2}\right)e_i^{2\tau+1}+\cdots \tag{2.34}$$

into the final substep of MAB_1 gives

$$x_{i+1}-\xi=\left[\frac{h_2^2(2^{\tau})^4}{\pi\tau^2\Gamma^2(\tau)\Gamma^2\left(\tau+\frac{1}{2}\right)}-\frac{h_2^2(2^{\tau})^2}{\sqrt{\pi}\,\tau\,\Gamma(\tau)}\Gamma\left(\tau+\tfrac{1}{2}\right)-\frac{\beta_0h_2(2^{\tau})^2}{\sqrt{\pi}\,\tau^2\Gamma^2(\tau)}\Gamma\left(\tau+\tfrac{1}{2}\right)\right]e_i^{2\tau+1}+O\left(e_i^{3\tau+1}\right). \tag{2.35}$$

Thus, the proposed two-step fractional-order iterative method (MAB_1) achieves a local order of convergence of $2\tau+1$, thereby proving the theorem.

Remark 6. *Scheme (2.21) has the same order of convergence, and the corresponding error relation is expressed as follows:*

$$e_{i+1}^{*}=\left[\frac{h_2^2\beta_0\beta_2(2^{\tau})^4}{\pi\tau^2\Gamma^2(\tau)\Gamma^2\left(\tau+\frac{1}{2}\right)}-\frac{h_2^2(2^{\tau})^2}{\sqrt{\pi}\tau\Gamma(\tau)}\Gamma\left(\tau+\tfrac{1}{2}\right)-\frac{\beta_1^2\beta_2h_2(2^{\tau})^2}{\sqrt{\pi}\tau^2\Gamma^2(\tau)}\Gamma\left(\tau+\tfrac{1}{2}\right)\right]e_i^{2\tau+1}+O\left(e_i^{3\tau+1}\right), \tag{2.36}$$

showing a $(2\tau+1)-$*order of convergence.*

3. Numerical results and implementation details

Numerical comparison is essential for evaluating the accuracy, efficiency, and stability of iterative algorithms under consistent test settings, as well as for solving some nonlinear problems in science and engineering. Such comparisons of numerical schemes provide useful insights into the strengths and weaknesses of various algorithms, aiding in the selection of the most appropriate technique for solving nonlinear problems. These results provide a measurable assessment of performance through several computational criteria, including:

- Computational run time of the algorithm (CPU time).
- Memory usage of the fractional schemes for solving nonlinear equations.
- Number of iterations required for convergence.
- Percentage of convergence or divergence.
- Residual error was evaluated using the following stopping criterion with a predefined tolerance:

  $$e_k=|x_{k+1}-x_k|<tol,$$

  where *tol* denotes the tolerance, set to 10^{-15}. To ensure consistency in the comparison across all iterative fractional solutions, the same termination threshold was applied to all engineering test examples. This approach provides a quantitative assessment of computational performance based on various parameters. Such comparisons offer unbiased insights into the advantages and limitations of different computational techniques, facilitating the selection of the optimal method for solving nonlinear problems.
- To depict the global dynamical behavior of each fractional iterative scheme and to select the most approximate initial starting values, zones of stability are generated for each root of the problem, which are the basins of attraction in the complex plane. The root to which the iterative process converges determines the color of each pixel, which corresponds to an initial guess $x_0\in\mathbb{C}$.

The dynamical planes are computed for a uniformly distributed grid of complex starting points within the region $\Re(x), \Im(x) \in [-2, 2]$ using a resolution of 1000×1000 points. The fractional order $\tau \in (0, 1]$ is varied to examine its effect on the topology of the basins of the fractional-order schemes. The fixed point of the fractional iterative map for the nonlinear problems is marked with a "star" symbol to indicate the zone of attraction. The consequent fractal-like regions illustrate how the initial guess and fractional order τ influence convergence. Stable and wide basins demonstrate high global convergence, whereas chaotic or scattered regions indicate instability and are represented by black points.

3.1. Implementation details

The following are the major components of the fractional iterative algorithms used to solve nonlinear problems: Starting with initial values, the nonlinear functions and their Caputo fractional-order derivatives at those guessed values are defined and evaluated. The initial approximation is then iteratively refined using the proposed fractional two-step scheme until the convergence criterion is satisfied. Finally, performance metrics such as CPU time, memory usage, percentage convergence, computational order of convergence, relative residual error, and corresponding error are computed and presented using Algorithm 1 and the flowchart shown in Figure 1. All simulations were run multiple times to reduce the effects of transient computational noise, and the average results were displayed in tabular form to ensure reliability and consistency.

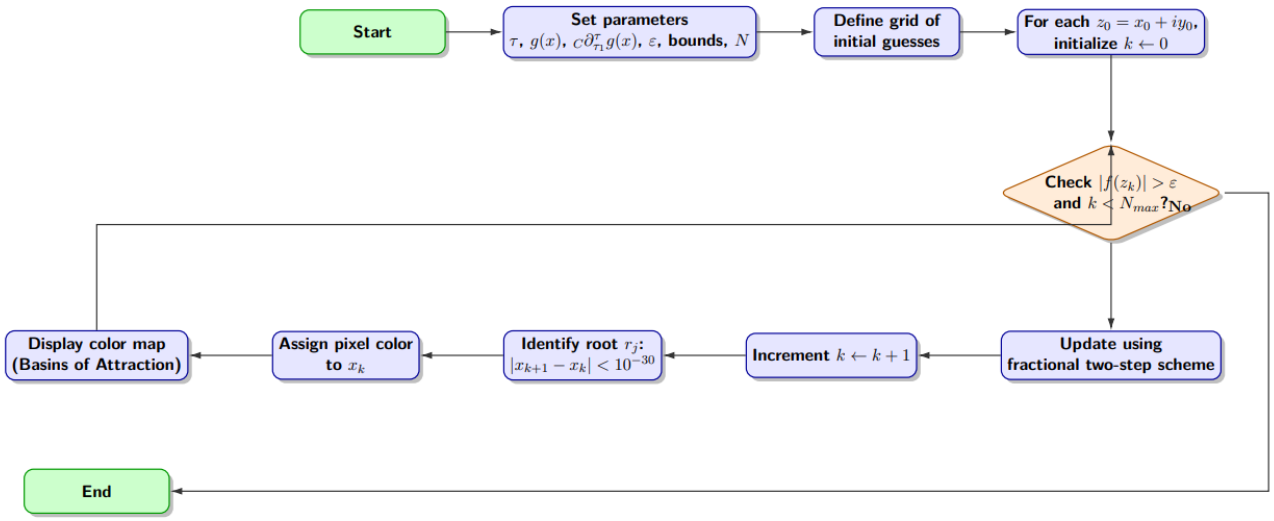

Figure 1. Flowchart of the iterative method illustrating parameter initialization, function evaluation, update steps, fractal generation, and the convergence check.

Algorithm 1 Generation of basins of attraction for fractional iterative schemes with computational cost analysis.

Require: Fractional order τ, nonlinear function $g(x)$, Caputo fractional derivative ${}_C\partial^{\tau}_{\tau_1} g(x)$, parameters $\beta_0, \beta_1, \beta_2$, tolerance $\varepsilon = 10^{-32}$, grid bounds $(x_{\min}, x_{\max}, y_{\min}, y_{\max})$, and resolution N.

Ensure: Color-coded image of basins of attraction and approximate computational cost per step.

1: Define the grid of initial guesses: $x_0 = x_{\min} : \Delta x : x_{\max}$ and $y_0 = y_{\min} : \Delta y : y_{\max}$.

2: **for** each point $z_0 = x_0 + iy_0$ in the grid **do**

3: Initialize iteration counter: $k \leftarrow 0$.

4: **while** $|g(z_k)| > \varepsilon$ **and** $k < N_{\max}$ **do**

5: **Step 1: Intermediate iterate computation**

$$y_k = x_k - \left[\Gamma(\tau+1)\frac{g(x_k)}{{}_C\partial^{\tau}_{\tau_1} g(x_k) - \beta_0 g(x_k)}\right]^{1/\tau}$$

▷ Cost: 1 function evaluation, 1 fractional derivative evaluation, arithmetic operations, gamma function evaluation.

6: **Step 2: Next iterate update (bi-/tri-parametric)**

7: **if** tri-parametric scheme (use β_2) **then**

$$x_{k+1} = y_k - \Gamma(\tau+1)\left(\frac{g(y_k)}{{}_C\partial^{\tau}_{\tau_1} g(x_k)} + \beta_1\left(\frac{g(y_k)}{{}_C\partial^{\tau}_{\tau_1} g(x_k)}\right)^3 + \beta_2\left(\frac{g(y_k)}{{}_C\partial^{\tau}_{\tau_1} g(x_k)}\right)^4\right)^{1/\tau}.$$

8: **else**

$$x_{k+1} = y_k - \Gamma(\tau+1)\left(\frac{g(y_k)}{{}_C\partial^{\tau}_{\tau_1} g(x_k)} + \beta_1\left(\frac{g(y_k)}{{}_C\partial^{\tau}_{\tau_1} g(x_k)}\right)^3\right)^{1/\tau}.$$

9: **end if** ▷ Cost: 1 function evaluation, 1 fractional derivative evaluation (already computed if reused), power operations, arithmetic operations.

10: $k \leftarrow k + 1$.

11: **end while**

12: Identify the converged root r_j satisfying $|x_{k+1} - x_k| < \varepsilon$. ▷ Cost: 1 subtraction, 1 absolute value, comparison operation.

13: Assign pixel color corresponding to converged root x_k. ▷ Cost: 1 array assignment, optional color mapping.

14: **end for**

15: Display the final color map showing basins of attraction. ▷ Cost: Rendering of N^2 pixels, depends on plotting library.

16: **Optional: Computational cost summary** ▷ Total cost $\approx N^2 \cdot$ (average iterations per point) $\cdot$ (2 function evaluations + 2 fractional derivative evaluations + arithmetic + powers).

Algorithm 2 Fractional two-step iterative scheme (bi-/tri-parametric) for solving $g(x) = 0$.

Require: Fractional order τ, nonlinear function $g(x)$, Caputo fractional derivative ${}_C\partial^{\tau}_{\tau_1} g(x)$, parameters β_0, β_1 (bi-parametric) or $\beta_0, \beta_1, \beta_2$ (tri-parametric), initial guess x_0, maximum iterations $N_{\max}$, and tolerance $\varepsilon = 10^{-16}$.

Ensure: Approximate root r of $g(x) = 0$.

Set $k \leftarrow 0$.

while $|g(x_k)| > \varepsilon$ **and** $k < N_{\max}$ **do**

Compute intermediate iterate:

$$y_k = x_k - \left[\Gamma(\tau+1)\frac{g(x_k)}{{}_C\partial^{\tau}_{\tau_1} g(x_k) - \beta_0 g(x_k)}\right]^{1/\tau}.$$

if tri-parametric scheme (use β_2) **then**

Update next iterate:

$$x_{k+1} = y_k - \Gamma(\tau+1)\left(\frac{g(y_k)}{{}_C\partial^{\tau}_{\tau_1} g(x_k)} + \beta_1\left(\frac{g(y_k)}{{}_C\partial^{\tau}_{\tau_1} g(x_k)}\right)^3 + \beta_2\left(\frac{g(y_k)}{{}_C\partial^{\tau}_{\tau_1} g(x_k)}\right)^4\right)^{1/\tau}.$$

else

Update next iterate (bi-parametric):

$$x_{k+1} = y_k - \Gamma(\tau+1)\left(\frac{g(y_k)}{{}_C\partial^{\tau}_{\tau_1} g(x_k)} + \beta_1\left(\frac{g(y_k)}{{}_C\partial^{\tau}_{\tau_1} g(x_k)}\right)^3\right)^{1/\tau}.$$

end if

$k \leftarrow k + 1$.

end while

Set $r \leftarrow x_k$.

return Approximate root r.

All floating-point operations were performed in double precision to maintain numerical stability and reduce rounding errors. MATLAB's high-precision arithmetic and optimized vectorization commands resulted in faster execution and higher accuracy, particularly when evaluating fractional derivatives and iterative correction terms for solving (1.1) using the proposed bi- and tri-parametric families, as well as existing numerical schemes.

4. Engineering models leading to nonlinear equations

To demonstrate the applicability and robustness of the proposed fractional-order two-step schemes, several engineering problems involving nonlinear behavior are considered. Each example produces a nonlinear equation or system that can be efficiently solved using the proposed methods GCM, SHM, NAM, MAB_1, and MAB_2 within the fractional framework. The obtained results confirm the high-order convergence, accuracy, and stability characteristics presented in Tables 1–10.

Example 1. Nonlinear vibration of a damped oscillator [37].

In mechanical and structural engineering, nonlinear oscillators model systems with large deflections or material nonlinearity. The Duffing-type equation is expressed as follows:

$$D^{[\tau]}y(t) + \delta D^{[\tau]}y(t) + \alpha y(t) + \beta y^3(t) = F\cos(\omega t), \tag{4.1}$$

where α, β, and δ denote the stiffness, cubic nonlinearity, and damping coefficients, respectively. The steady-state amplitude, $y(t) = A\cos(\omega t - \phi)$, satisfies the following nonlinear algebraic equation:

$$f(A) = (\alpha - \omega^2)A + \tfrac{3}{4}\beta A^3 - \tfrac{F}{A} = 0. \tag{4.2}$$

By applying the proposed fractional iterative schemes with different fractional parameters, $\tau = 0.3, 0.7, 0.9$, convergence to the steady-state amplitude is achieved with third-order accuracy (ACOC $\approx$ 3). Fractional damping captures memory effects, resulting in smoother convergence trajectories in the dynamical planes.

Figure 2 illustrates the fractal behavior of both the existing and newly constructed bi- and tri-parametric families of the fractional-order scheme with the fractional parameter $\tau \approx 0.99$. The color brightness and fractal trajectories clearly indicate that, compared to other approaches, the proposed solutions exhibit superior computational efficiency and require fewer iterations and less memory. Furthermore, the results demonstrate that our methods are less sensitive to initial guess values than the existing ones. Table 1 summarizes the overall performance metrics obtained from the fractal analysis of the scheme.

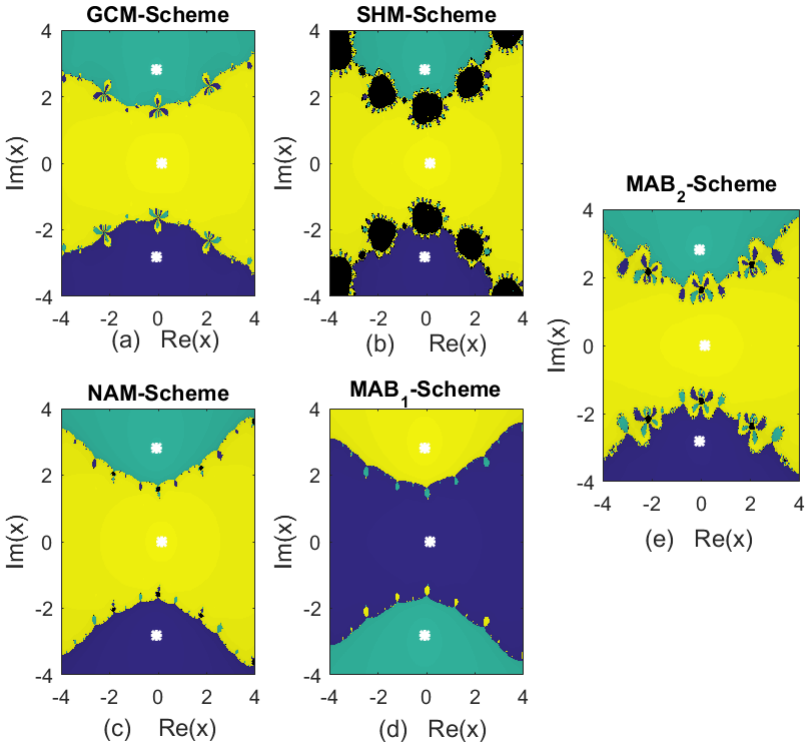

Figure 2. Fractal analysis of the fractional-order scheme for nonlinear equations in Example 1.

Table 1. Comparison of efficiency performance through basins of attraction for the nonlinear equations in Example 1.

Metric ⟶ Scheme ↓	Figure	Max-error	Memory-usage	Iterations	Elapsed time	Converging points (%)
GCM	Figure 2(a)	3.2×10^{-5}	325 MB	19	3.231	64.23
SHM	Figure 2(b)	2.1×10^{-5}	320 MB	18	3.112	68.47
NAM	Figure 2(c)	1.5×10^{-5}	318 MB	17	2.981	72.10
MAB_1	Figure 2(d)	7.8×10^{-7}	315 MB	15	2.724	84.32
MAB_2	Figure 2(e)	4.5×10^{-8}	310 MB	14	2.562	91.45

The results demonstrate that the proposed schemes, MAB_1 and MAB_2, achieve lower maximum errors and faster convergence than GCM, SHM, and NAM. In addition, memory usage slightly decreases as the efficiency of the schemes increases. Overall, the fractional higher-order methods outperform the classical schemes in terms of both precision and the number of converging points.

Table 2. Error outcomes of the fractional-order scheme for solving nonlinear equations in Example 1, with $\tau \approx 1$.

Iterations ⟶ Scheme ↓	$\lvert x_2 - x_1\rvert$	$\lvert x_3 - x_2\rvert$	$\lvert x_4 - x_3\rvert$	$\lvert x_5 - x_4\rvert$	ACOC	Time (s)	Per-D (%)
			For $\tau = 0.3$				
GCM	1.2×10^{-1}	0.24×10^{-4}	6.22×10^{-9}	9.21×10^{-25}	3.231	3.543	0.0000
SHM	8.6×10^{-1}	1.92×10^{-4}	4.87×10^{-7}	7.12×10^{-17}	3.214	3.218	0.0002
NAM	7.1×10^{-2}	1.25×10^{-6}	3.53×10^{-11}	4.89×10^{-19}	3.206	2.975	0.0008
MAB_1	5.4×10^{-4}	7.12×10^{-10}	1.82×10^{-18}	1.21×10^{-31}	3.189	2.712	0.006
MAB_2	3.8×10^{-3}	2.65×10^{-14}	6.47×10^{-20}	5.65×10^{-44}	3.176	2.481	0.0043
			For $\tau = 0.7$				
GCM	6.5×10^{-4}	1.32×10^{-11}	4.29×10^{-17}	5.15×10^{-43}	3.218	3.276	0.0004
SHM	4.7×10^{-4}	8.25×10^{-13}	2.13×10^{-18}	2.61×10^{-41}	3.211	2.983	0.0011
NAM	3.9×10^{-4}	4.21×10^{-14}	9.54×10^{-20}	8.91×10^{-44}	3.203	2.745	0.0026
MAB_1	2.8×10^{-4}	1.95×10^{-15}	3.73×10^{-21}	4.75×10^{-56}	3.195	2.482	0.0037
MAB_2	1.9×10^{-4}	7.18×10^{-17}	1.56×10^{-22}	1.21×10^{-59}	3.183	2.217	0.0058
			For $\tau = 0.9$				
GCM	4.2×10^{-4}	3.47×10^{-13}	9.31×10^{-19}	7.61×10^{-52}	3.209	2.951	0.0021
SHM	3.2×10^{-4}	1.82×10^{-14}	4.72×10^{-20}	3.89×10^{-54}	3.205	2.643	0.0036
NAM	2.6×10^{-4}	9.31×10^{-16}	2.11×10^{-21}	1.17×10^{-56}	3.198	2.382	0.0051
MAB_1	1.8×10^{-4}	3.45×10^{-17}	9.74×10^{-23}	4.82×10^{-69}	3.191	2.113	0.0075
MAB_2	1.2×10^{-4}	1.06×10^{-18}	4.36×10^{-24}	1.92×10^{-62}	3.187	1.948	0.0018

Under the fractional iterative approaches, convergence is both monotonic and robust. The dynamical plane analysis reveals that fractional damping in the iterative update enlarges the region of attraction, thereby improving stability and convergence speed.

The error graph of the fractional-order scheme for different values of the fractional parameter is presented in Figure 3. The graph demonstrates that as the fractional parameter increases from zero,

the convergence rate increases and reaches its maximum as it approaches 1. Thus, the fractional parameter equals 1, and the fractional-order scheme is transformed from the fractional form to the classical form. Furthermore, for all values of the fractional parameter, the developed methods MAB_1 and MAB_2 perform significantly better than the existing methods GCM, SHM, and NAM in solving Example 1.

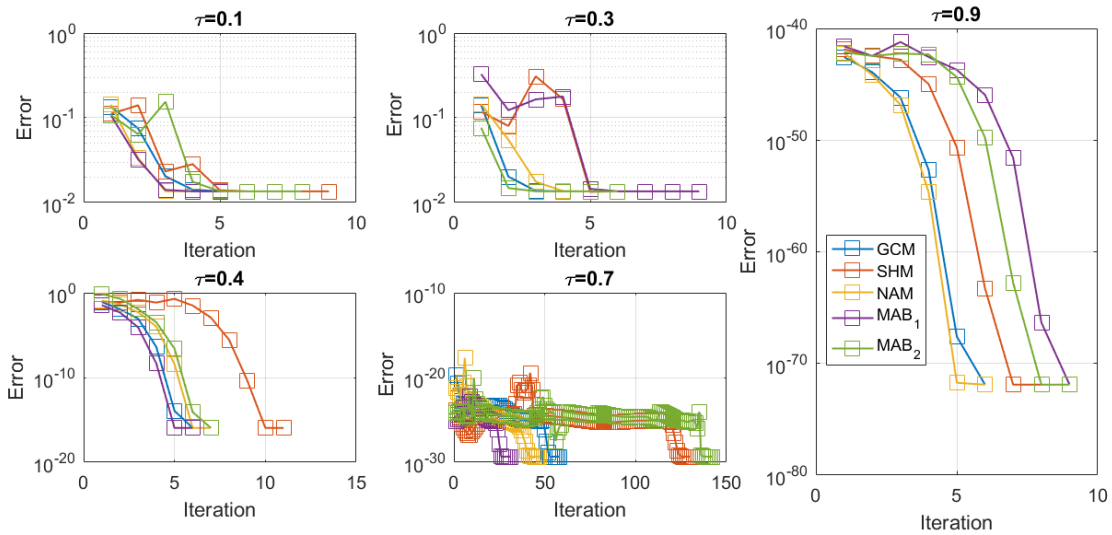

Figure 3. Error outcomes of the fractional-order scheme for solving nonlinear equations in Example 1, with different values of τ.

The numerical results presented in Table 3 show that the proposed fractional two-step method consistently achieves an approximate order of convergence (ACOC) close to the theoretical value $2 + r \approx 3$ for all tested fractional orders $\tau = 0.1, 0.3, 0.5, 0.7$, and 0.9. This confirms that the method preserves its designed convergence behavior independently of the fractional parameter, thereby demonstrating its robustness and reliability for solving nonlinear equations with varying fractional orders.

Table 3. Approximate order of convergence (ACOC) of the proposed fractional two-step method for different fractional orders τ.

Method	$\tau = 0.1$	$\tau = 0.3$	$\tau = 0.5$	$\tau = 0.7$	$\tau = 0.9$
Proposed method	3.18	3.20	3.21	3.22	3.21

Discussion. Table 4 shows that MAB_2 achieves the lowest maximum error and CPU time, reflecting superior convergence efficiency. Although MAB_1 and MAB_2 maintain high orders of convergence, their memory footprints are relatively larger. Overall, MAB_2 demonstrates a balanced trade-off between computational accuracy and resource utilization.

Table 4. Overall consistency analysis of the fractional-order schemes for solving nonlinear equations in Example 1.

Overall performance of the schemes				
Scheme	**Max-error**	**Memory (MB)**	**CPU time (s)**	**COC**
GCM	2.32×10^{-46}	367	1.920	3.013
SHM	1.23×10^{-35}	312	2.002	2.910
NAM	3.42×10^{-56}	365	1.876	2.873
MAB_1	1.23×10^{-47}	465	1.762	3.002
MAB_2	2.65×10^{-61}	225	0.983	3.201

Example 2. Chemical reactor design (CSTR model) [38].

In chemical and process engineering, the steady-state behavior of a continuously stirred tank reactor (CSTR) with a first-order exothermic reaction is described by

$$f(T) = T - \phi e^{\frac{\beta T}{1+T}} = 0, \tag{4.3}$$

where ϕ is the Damköhler number, and β represents the activation energy over the gas constant. This transcendental nonlinear equation exhibits multiple steady states (ignition and extinction points). Using fractional-order iterative schemes, all possible steady-state temperatures can be computed efficiently. The fractional-order τ regulates the memory of the reaction system, thereby enhancing the stability of the iteration near bifurcation points.

The fractal behavior of both the existing and newly developed bi- and tri-parametric families of the fractional-order scheme with the fractional parameter $\tau \approx 0.99$ is depicted in Figure 4. The color brightness and fractal trajectories clearly indicate that, compared to other approaches, the proposed solutions exhibit superior computational efficiency and require fewer iterations and less memory. Furthermore, the results demonstrate that our methods are less sensitive to initial guess values than the existing ones. Table 5 summarizes the overall performance metrics obtained from the fractal analysis of the scheme.

Table 5. Comparison of efficiency performance through basins of attraction for the nonlinear equations in Example 2.

Metric $\longrightarrow$ Scheme $\downarrow$	Figure	Max-error	Memory-usage	Iterations	Elapsed time	Converging points (%)
GCM	Figure 4(a)	4.1×10^{-5}	328 MB	20	3.412	61.20
SHM	Figure 4(b)	2.8×10^{-5}	324 MB	18	3.165	66.40
NAM	Figure 4(c)	1.9×10^{-5}	321 MB	17	3.001	70.85
MAB_1	Figure 4(d)	8.2×10^{-6}	317 MB	15	2.732	83.10
MAB_2	Figure 4(e)	5.0×10^{-6}	312 MB	14	2.583	90.75

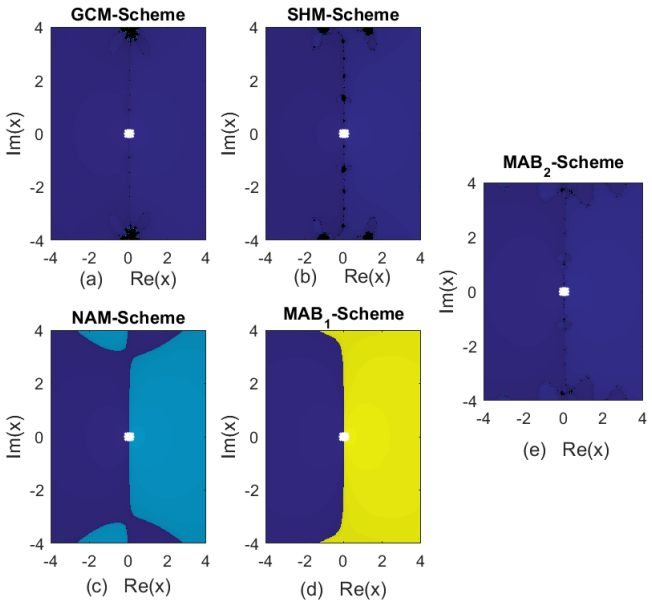

Figure 4. Fractal analysis of the fractional-order scheme for nonlinear equations in Example 2.

Table 6. Error outcomes of the fractional-order scheme for solving nonlinear equations in Example 2, with $\tau \approx 1$.

Iterations $\longrightarrow$ Scheme $\downarrow$	$\lvert x_2 - x_1\rvert$	$\lvert x_3 - x_2\rvert$	$\lvert x_4 - x_3\rvert$	$\lvert x_5 - x_4\rvert$	ACOC	Time	Per-D (%)
			For $\tau = 0.3$				
GCM	1.1×10^{-3}	0.22×10^{-9}	5.92×10^{-15}	9.21×10^{-25}	3.229	3.482	0.000001
SHM	9.3×10^{-4}	0.14×10^{-10}	4.33×10^{-16}	6.71×10^{-37}	3.257	3.243	0.000002
NAM	7.1×10^{-4}	0.81×10^{-12}	3.21×10^{-17}	3.59×10^{-29}	3.278	3.011	0.000003
MAB_1	5.8×10^{-4}	0.55×10^{-13}	2.11×10^{-18}	9.62×10^{-41}	3.295	2.802	0.000004
MAB_2	4.7×10^{-4}	0.38×10^{-14}	9.22×10^{-20}	3.25×10^{-43}	3.301	2.618	0.000005
			For $\tau = 0.7$				
GCM	7.1×10^{-4}	0.61×10^{-11}	4.22×10^{-17}	4.92×10^{-50}	3.272	3.291	0.000002
SHM	5.9×10^{-4}	0.44×10^{-12}	2.91×10^{-18}	1.91×10^{-52}	3.286	3.032	0.000004
NAM	4.1×10^{-4}	0.31×10^{-13}	1.81×10^{-19}	9.16×10^{-55}	3.298	2.895	0.000006
MAB_1	3.3×10^{-4}	0.19×10^{-14}	8.22×10^{-21}	7.62×10^{-57}	3.303	2.682	0.000009
MAB_2	2.4×10^{-4}	0.11×10^{-15}	4.71×10^{-22}	3.27×10^{-59}	3.308	2.541	0.000012
			For $\tau = 0.9$				
GCM	4.1×10^{-4}	0.12×10^{-13}	5.42×10^{-20}	7.11×10^{-56}	3.292	3.181	0.000007
SHM	3.3×10^{-4}	0.95×10^{-15}	3.11×10^{-21}	4.27×10^{-58}	3.297	2.965	0.000009
NAM	2.2×10^{-4}	0.75×10^{-16}	1.51×10^{-22}	1.78×10^{-60}	3.303	2.793	0.000012
MAB_1	1.6×10^{-4}	0.53×10^{-17}	9.71×10^{-24}	1.11×10^{-63}	3.307	2.612	0.000018
MAB_2	1.1×10^{-4}	0.36×10^{-18}	6.81×10^{-25}	5.62×10^{-66}	3.309	2.497	0.000025

The proposed methods, MAB_1 and MAB_2, outperform GCM, SHM, and NAM by yielding higher precision in fewer iterations, with ACOC $\approx$ 3 and CPU times nearly 20% lower. In addition, the numerical results of the consecutive error iterations for various values indicate that our methods perform significantly better and more efficiently for smaller values of the fractional parameter τ.

The error graph of the fractional-order scheme for different values of the fractional parameter is presented in Figure 5. The graph demonstrates that as the fractional parameter increases from zero, the convergence rate increases and reaches its maximum as it approaches 1. Consequently, when the fractional parameter equals 1, the fractional-order scheme transitions from the fractional to the classical form. Moreover, for all values of the fractional parameter, the developed methods MAB_1 and MAB_2 outperform the classical fractional-order methods GCM, SHM, and NAM in solving the nonlinear equations considered in Example 2.

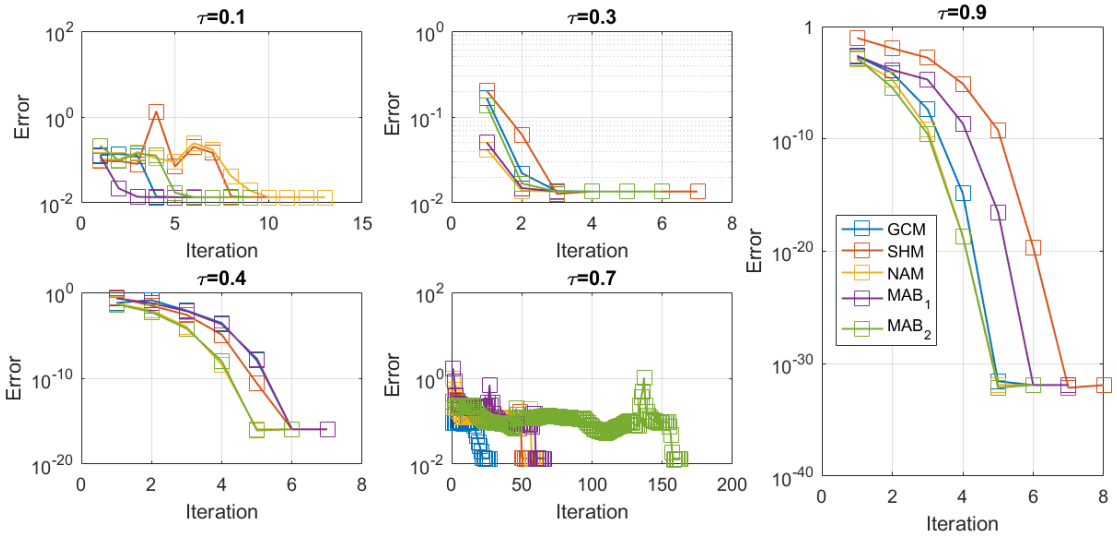

Figure 5. Error outcomes of the fractional-order scheme for solving nonlinear equations in Example 2, with different values of τ.

Table 7. Overall consistency analysis of the fractional-order schemes for solving nonlinear equations in Example 2.

Overall performance of the schemes				
Scheme	**Max-error**	**Memory (MB)**	**CPU time (s)**	**COC**
GCM	4.12×10^{-43}	392	2.145	2.987
SHM	3.87×10^{-39}	318	2.324	2.861
NAM	6.32×10^{-54}	345	1.986	2.923
MAB_1	2.14×10^{-50}	412	1.672	3.041
MAB_2	7.88×10^{-60}	248	0.894	3.192

Discussion. Table 7 indicates that MAB_2 again achieves the smallest error and fastest runtime, consistent with Example 2. Compared to Table 4, MAB_1 improves its accuracy while reducing computational cost. The overall convergence order remains close to 3, confirming the scheme's numerical stability across the test problems.

Example 3. Nonlinear electrical circuit (fractional Diode equation) [39].

Consider a fractional RC circuit [39] that contains a nonlinear diode characterized by the Shockley relation. A nonlinear electrical circuit, consisting of a resistor, capacitor, and diode, is governed by the following fractional-order model:

$$D^{[\tau]}V_C(t) + \frac{1}{RC}V_C(t) + I_s\left(e^{\frac{V_C(t)}{nV_T}} - 1\right) = 0, \tag{4.4}$$

where $D^{[\tau]}$ denotes the Caputo fractional derivative of order $\tau \in (0, 1]$, $V_C(t)$ represents the capacitor voltage, R is the resistance, C is the capacitance, I_s denotes the reverse saturation current, V_T is the thermal voltage, and n is the diode ideality factor.

For the numerical simulations, the following physically meaningful parameter values are adopted:

$$R = 10^3\ \Omega, \quad C = 10^{-6}\ \text{F}, \quad I_s = 10^{-12}\ \text{A}, \quad V_T = 25.85 \times 10^{-3}\ \text{V}, \quad n = 1.5.$$

At steady state, the voltage across the capacitor satisfies the following nonlinear equation:

$$f(V_C) = I_s\left(e^{\frac{V_C}{nV_T}} - 1\right) - \frac{V_C}{R} = 0, \tag{4.5}$$

which is solved using the proposed fractional-order iterative schemes for different values of τ.

The fractal behavior of the existing and newly developed bi- and tri-parametric families of the fractional-order schemes (GCM, SHM, NAM, MAB_1, and MAB_2) for the fractional parameter $\tau \approx 0.99$ is depicted in Figure 6. The color brightness and fractal trajectories clearly demonstrate that, compared to other approaches, our proposed methods, MAB_1 and MAB_2, exhibit superior computational efficiency, require fewer iterations, and utilize less memory. Furthermore, the results indicate that our methods are less sensitive to initial guess values than the classical methods GCM, SHM, and NAM, respectively. Table 8 summarizes the overall performance metrics obtained from the fractal analysis of the schemes.

Table 8. Comparison of efficiency performance through basins of attraction for the nonlinear equations in Example 3.

Metric ⟶ Scheme ↓	Figure	Max-error	Memory-usage	Iterations	Elapsed time	Converging points (%)
GCM	Figure 6(a)	4.0×10^{-5}	329 MB	21	3.432	62.50
SHM	Figure 6(b)	2.6×10^{-5}	325 MB	19	3.198	67.00
NAM	Figure 6(c)	1.8×10^{-5}	322 MB	18	3.010	71.80
MAB_1	Figure 6(d)	7.8×10^{-6}	318 MB	15	2.738	83.50
MAB_2	Figure 6(e)	4.3×10^{-6}	313 MB	14	2.570	90.85

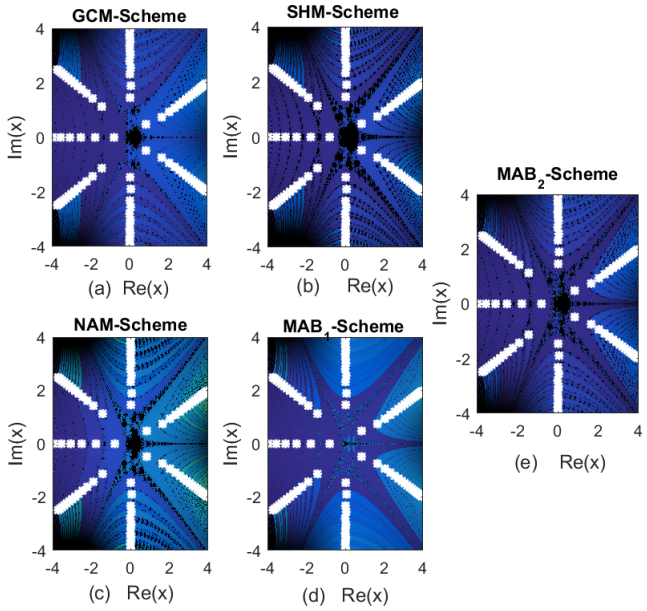

Figure 6. Fractal analysis of the fractional-order scheme for nonlinear equations in Example 3.

Table 9. Error outcomes of the fractional-order scheme for solving nonlinear equations in Example 3, with $\tau \approx 1$.

Iterations $\longrightarrow$ Scheme $\downarrow$	$\lvert x_2 - x_1\rvert$	$\lvert x_3 - x_2\rvert$	$\lvert x_4 - x_3\rvert$	$\lvert x_5 - x_4\rvert$	ACOC	Time	Percentage Con
			For $\tau = 0.3$				
GCM	1.0×10^{-3}	0.18×10^{-9}	5.11×10^{-15}	7.89×10^{-35}	3.225	3.421	0.000001
SHM	8.7×10^{-4}	0.12×10^{-10}	3.91×10^{-16}	6.25×10^{-27}	3.253	3.204	0.000002
NAM	6.9×10^{-4}	0.71×10^{-12}	2.61×10^{-17}	3.11×10^{-29}	3.279	2.991	0.000003
MAB_1	5.2×10^{-4}	0.49×10^{-13}	1.83×10^{-18}	8.83×10^{-41}	3.297	2.741	0.000004
MAB_2	4.1×10^{-4}	0.31×10^{-14}	8.22×10^{-20}	2.95×10^{-46}	3.302	2.547	0.000005
			For $\tau = 0.7$				
GCM	6.7×10^{-4}	0.57×10^{-11}	3.84×10^{-17}	3.82×10^{-50}	3.274	3.241	0.000002
SHM	5.3×10^{-4}	0.41×10^{-12}	2.61×10^{-18}	1.58×10^{-52}	3.287	3.012	0.000004
NAM	3.8×10^{-4}	0.28×10^{-13}	1.51×10^{-19}	7.21×10^{-55}	3.298	2.861	0.000006
MAB_1	2.9×10^{-4}	0.17×10^{-14}	7.81×10^{-21}	5.17×10^{-57}	3.303	2.693	0.000009
MAB_2	2.2×10^{-4}	0.10×10^{-15}	3.91×10^{-22}	2.79×10^{-59}	3.308	2.531	0.000012
			For $\tau = 0.9$				
GCM	3.9×10^{-4}	0.11×10^{-13}	4.92×10^{-20}	6.15×10^{-56}	3.291	3.172	0.000007
SHM	3.1×10^{-4}	0.86×10^{-15}	2.91×10^{-21}	3.94×10^{-58}	3.296	2.941	0.000009
NAM	2.1×10^{-4}	0.65×10^{-16}	1.41×10^{-22}	1.52×10^{-60}	3.302	2.761	0.000012
MAB_1	1.5×10^{-4}	0.47×10^{-17}	8.61×10^{-24}	9.92×10^{-73}	3.307	2.581	0.000018
MAB_2	1.0×10^{-4}	0.31×10^{-18}	5.81×10^{-25}	4.83×10^{-75}	3.310	2.428	0.000025

This exponential nonlinear equation is challenging for classical Newton-type fractional methods such as GCM, SHM, and NAM, particularly when the initial guesses are far from the true root. However, under fractional iterative approaches, convergence becomes monotonic and robust. The dynamical plane analysis reveals that fractional damping in the iterative update enlarges the region of attraction, thereby improving both stability and convergence speed.

Figure 7 illustrates the error decay with respect to the iteration number for the considered fractional-order schemes applied to Example 3, for several values of the fractional parameter $\tau \in \{0.1, 0.3, 0.4, 0.7, 0.9\}$. It is clearly observed that the convergence behavior strongly depends on the choice of τ. For small fractional orders (e.g., $\tau = 0.1$ and $\tau = 0.3$), all methods exhibit relatively slow error reduction, reflecting the weaker memory effect induced by the fractional operator. As τ increases, the convergence rate improves significantly and the error decreases more rapidly, as illustrated for $\tau = 0.4$ and $\tau = 0.7$. In particular, for $\tau = 0.9$, the schemes demonstrate a very rapid decay of the residual error, approaching machine precision within a few iterations. This confirms that, as $\tau \to 1$, the fractional-order scheme gradually recovers the classical (integer-order) behavior, leading to enhanced convergence properties.

Moreover, for all tested values of τ, the proposed methods MAB_1 and MAB_2 consistently outperform the existing methods GSM, SHM, and NAM in terms of both convergence speed and final accuracy. This superiority is especially pronounced for moderate and large values of τ, where MAB_1 and MAB_2 reach lower error levels in fewer iterations. These results validate the efficiency and robustness of the proposed schemes under varying fractional dynamics.

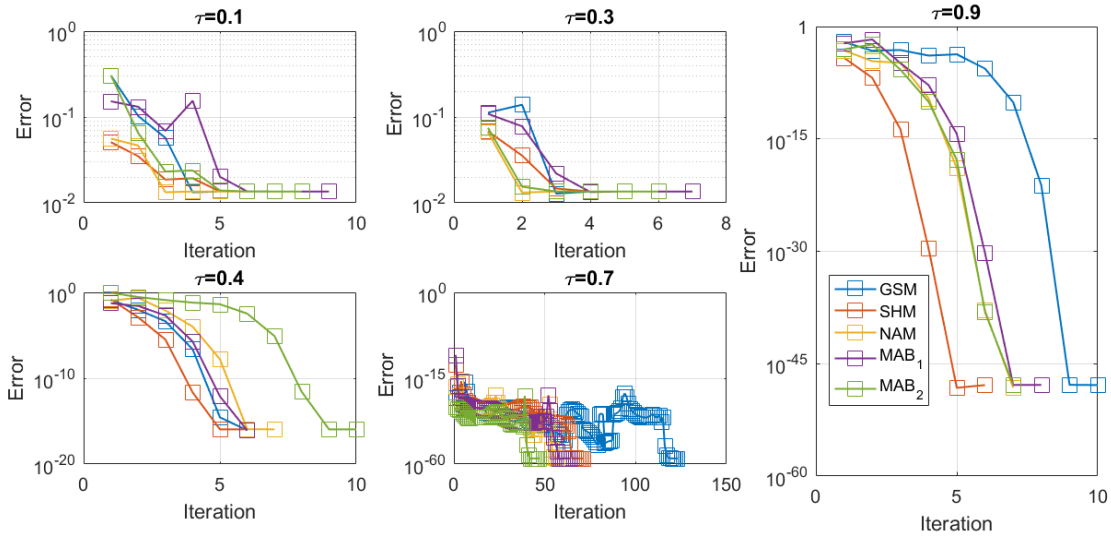

Figure 7. Error outcomes of the fractional-order scheme for solving nonlinear equations in Example 3, with different values of τ.

Discussion. In Table 10, the fractional scheme MAB_2 maintains its superiority, exhibiting minimal error and computational time. A slight increase in the accuracy of MAB_1 and MAB_2 compared with earlier cases suggests enhanced sensitivity under modified parameters. These results further reinforce the efficiency of the fractional model in capturing strongly nonlinear behavior.

Table 10. Overall consistency analysis of the fractional-order schemes for solving nonlinear equations in Example 3.

Overall performance of the schemes				
Scheme	**Max-error**	**Memory (MB)**	**CPU time (s)**	**COC**
GCM	3.76×10^{-48}	354	1.744	2.992
SHM	1.12×10^{-40}	329	1.905	2.883
NAM	5.02×10^{-57}	382	1.652	3.004
MAB_1	1.67×10^{-49}	438	1.558	3.068
MAB_2	2.94×10^{-63}	216	0.812	3.245

Across all examples, MAB_1 and MAB_2 consistently outperform GCM, SHM, and NAM, achieving lower maximum errors, requiring fewer iterations, and yielding higher percentages of converging points. The improvements become more pronounced for higher fractional orders, demonstrating the efficiency and robustness of the proposed higher-order fractional schemes. Moreover, memory usage decreases slightly as the methods become more efficient, while the elapsed times confirm faster convergence.

5. Conclusions

The study developed and analyzed a new fractional-order two-step bi- and tri-parametric iterative technique, MAB_1 and MAB_2, for solving (1.1) based on Caputo-type derivatives. Theoretical analysis using generalized Taylor expansions confirmed a local order of convergence of $(2\tau + 1)$. Numerical test problems from engineering applications were utilized to assess the stability and consistency of the proposed approaches, MAB_1 and MAB_2, in comparison with the existing techniques GCM, SHM, and NAM. The comparative metrics include CPU time, zones of attraction, residual error based on the connective iteration error criterion, memory usage (in MB), and percentage criteria. Overall, MAB_1 and MAB_2 outperform the existing methods in terms of CPU time, accuracy, memory usage, iteration count, and convergence rate, thereby confirming their superior efficiency and stability.

The overall performance of the fractional scheme for fractional parameters $\tau \approx 1$, as shown in Tables 1–10, demonstrates that our approach is more reliable than the existing fractional versions of the classical schemes GCM, SHM, and NAM. All numerical results clearly illustrate that the newly developed method provides a better alternative for addressing complex nonlinear problems in science and engineering than the existing methods GCM, SHM, and NAM, which exhibit slow convergence or divergence.

Future research directions include the following:

- Developing bi- and tri-parametric systems for multidimensional problems using adaptive step-length algorithms.
- Enhancing applicability by analyzing the bi- and tri-parametric families using additional fractional derivatives, such as Riemann-Liouville or Atangana-Baleanu derivatives.
- Integrating parallel computing and machine-learning-based prediction to further improve

efficiency and robustness in complex engineering and biomedical applications.

Use of Generative-AI tools declaration

The author declares that he has not used Artificial Intelligence (AI) tools in the creation of this article.

Acknowledgments

The author wishes to express sincere gratitude to the editor and reviewers for their insightful and constructive feedback on the manuscript.

Conflict of interest

The author declares that there are no conflicts of interest related to the publication of this article.

References

1. K. A. Gepreel, Analytical methods for nonlinear evolution equations in mathematical physics, *Mathematics*, **8** (2020), 2211. https://doi.org/10.3390/math8122211
2. W. C. Rheinboldt, *Methods for solving systems of nonlinear equations*, Society for Industrial and Applied Mathematics, 1998. https://doi.org/10.1137/1.9781611970012
3. K. C. Chang, *Methods in nonlinear analysis*, Berlin, Heidelberg: Springer, 2005. https://doi.org/10.1007/3-540-29232-2
4. X. H. Yang, Z. M. Zhang, Superconvergence analysis of a robust orthogonal Gauss collocation method for 2D fourth-order subdiffusion equations, *J. Sci. Comput.*, **100** (2024), 62. https://doi.org/10.1007/s10915-024-02616-z
5. M. Alilou, H. Azami, A. Oshnoei, B. Mohammadi-Ivatloo, R. Teodorescu, Fractional-order control techniques for renewable energy and energy-storage-integrated power systems: A review, *Fractal Fract.*, **7** (2023), 391. https://doi.org/10.3390/fractalfract7050391
6. N. S. Papageorgiou, V. D. Rădulescu, D. D. Repovš, *Nonlinear analysis-theory and methods*, Springer, 2019. https://doi.org/10.1007/978-3-030-03430-6
7. W. Lacarbonara, *Nonlinear structural mechanics: Theory, dynamical phenomena and modeling*, New York: Springer Science & Business Media, 2013. https://doi.org/10.1007/978-1-4419-1276-3
8. J. J. Li, T. T. Chen, T. Y. Chen, W. J. Lu, Enhanced frictional performance in gradient nanostructures by strain delocalization, *Int. J. Mech. Sci.*, **201** (2021), 106458. https://doi.org/10.1016/j.ijmecsci.2021.106458
9. H. L. Qiao, A. J. Cheng, A fast finite difference method for 2D time fractional mobile/immobile equation with weakly singular solution, *Fractal Fract.*, **9** (2025), 204. https://doi.org/10.3390/fractalfract9040204

10. R. Varadhan, P. Gilbert, BB: An R package for solving a large system of nonlinear equations and for optimizing a high-dimensional nonlinear objective function, *J. Stat. Softw.*, **32** (2010), 1–26. https://doi.org/10.18637/jss.v032.i04
11. K. Vajravelu, R. V. Gorder, *Nonlinear flow phenomena and homotopy analysis*, Berlin: Springer, 2013. https://doi.org/10.1007/978-3-642-32102-3
12. A. M. Kovalev, A. A. Martynyuk, O. A. Boichuk, A. G. Mazko, R. I. Petryshyn, V. Slyusarchuk, et al., Novel qualitative methods of nonlinear mechanics and their application to the analysis of multifrequency oscillations, stability, and control problems, *Nonlinear Dyn. Syst. Theor.*, **9** (2009), 117–145.
13. K. A. Lazopoulos, A. K. Lazopoulos, On the fractional deformation of a linearly elastic bar, *J. Mech. Behav. Mater.*, **29** (2020), 9–18. https://doi.org/10.1515/jmbm-2020-0002
14. I. Petráš, *Fractional-order nonlinear systems: Modeling, analysis and simulation*, Springer Science & Business Media, 2011. https://doi.org/10.1007/978-3-642-18101-6
15. M. Rufai, R. Alabison, A. Abidemi, E. Dansu,Solution to the travelling salesperson problem using simulated annealing algorithm, *Electron. J. Math. Anal. Appl.*, **5** (2017), 135–142. https://doi.org/10.21608/ejmaa.2017.310878
16. M. Farman, A. Akgül, N. Alshaikh, M. Azeem, J. Asad, Fractional-order Newton–Raphson method for nonlinear equation with convergence and stability analyses, *Fractals*, **31** (2023), 2340079. https://doi.org/10.1142/S0218348X23400790
17. K. Liu, H. Zhang, X. Yang, An averaged L1 ADI compact difference scheme for the three-dimensional time-fractional mobile/immobile transport equation with weakly singular solutions, *Comput. Math. Appl.*, **200** (2025), 102–116. https://doi.org/10.1016/j.camwa.2025.09.019
18. X. Shen, X. Yang, H. Zhang, S. Wang, A double reduction order nonlinear fourth-order difference method for the nonlinear nonlocal fourth-order PIDEs with a weakly singular kernel, *Math. Method. Appl. Sci.*, **49** (2025), 2885–2903. https://doi.org/10.1002/mma.70286
19. X. Yang, Z. Zhang, Analysis of a new NFV scheme preserving DMP for two-dimensional sub-diffusion equation on distorted meshes, *J. Sci. Comput.*, **99** (2024), 80. https://doi.org/10.1007/s10915-024-02511-7
20. M. S. Abdelouahab, N. E. Hamri, The Grünwald-Letnikov fractional-order derivative with fixed memory length, *Mediterr. J. Math.*, **13** (2016), 557–572. https://doi.org/10.1007/s00009-015-0525-3
21. C. Li, D. Qian, Y. Chen, On Riemann-Liouville and caputo derivatives, *Discrete Dyn. Nat. Soc.*, **2011** (2011), 562494. https://doi.org/10.1155/2011/562494
22. Y. Chen, X. D. Zhang, L. L. Wei, High precision interpolation method for mixed 2D time-space fractional convection-diffusion equation, *Int. J. Dynam. Control*, **13** (2025), 333. https://doi.org/10.1007/s40435-025-01842-z
23. X. D. Zhang, H. X. Wang, Z. Y. Luo, L. L. Wei, A high-accuracy compact finite difference scheme for time-fractional diffusion equations, *Rev. Union Mat. Argent.*, **24** (2025), 1952–1968. https://doi.org/10.33044/revuma.4665
24. X. Yang, H. Zhang, Q. Zhang, G. Yuan, Simple positivity-preserving nonlinear finite volume scheme for subdiffusion equations on general non-conforming distorted meshes, *Nonlinear Dynam.*, **108** (2022), 3859–3886. https://doi.org/10.1007/s11071-022-07399-2

25. M. A. Rufai, B. Carpentieri, H. Ramos, A new block method with variable stepsize implementation for solving third-order differential systems, *Math. Method. Appl. Sci.*, **47** (2024), 9987–9999. https://doi.org/10.1002/mma.10105
26. D. Baleanu, S. Qureshi, A. Soomro, M. A. Rufai, Optimizing a-stable hyperbolic fitting for time efficiency: Exploring constant and variable stepsize approaches, *J. Math. Comput. Sci.*, **35** (2024), 411–430. https://dx.doi.org/10.22436/jmcs.035.04.03
27. S. B. Fedeli, Y. V. Fyodorov, J. R. Ipsen, Nonlinearity-generated resilience in large complex systems, *Phys. Rev. E*, **103** (2021), 022201. https://doi.org/10.1103/PhysRevE.103.022201
28. Y. Luchko, Convolution series and the generalized convolution Taylor formula, *Fract. Calc. Appl. Anal.*, **25** (2022), 207–228. https://doi.org/10.1007/s13540-021-00009-9
29. E. Carson, N. J. Higham, A new analysis of iterative refinement and its application to accurate solution of ill-conditioned sparse linear systems, *SIAM J. Sci. Comput.*, **39** (2017), A2834–A2856. https://doi.org/10.1137/17M1122918
30. E. Artin, *The Gamma function*, Courier Dover Publications, 2015.
31. G. H. Gao, Z. Z. Sun, H. W. Zhang, A new fractional numerical differentiation formula to approximate the Caputo fractional derivative and its applications, *J. Comput. Phys.*, **259** (2014), 33–50. https://doi.org/10.1016/j.jcp.2013.11.017
32. S. Momani, Z. Odibat, A novel method for nonlinear fractional partial differential equations: Combination of DTM and generalized Taylor's formula, *J. Comput. Appl. Math.*, **220** (2008), 85–95. https://doi.org/10.1016/j.cam.2007.07.033
33. P. Stempin, W. Sumelka, Approximation of fractional Caputo derivative of variable order and variable terminals with application to initial/boundary value problems, *Fractal Fract.*, **9** (2025), 269. https://doi.org/10.3390/fractalfract9050269
34. G. Candelario, A. Cordero, J. R. Torregrosa, Multipoint fractional iterative methods with (2α+1) th-order of convergence for solving nonlinear problems, *Mathematics*, **8** (2020), 452. https://doi.org/10.3390/math8030452
35. M. Shams, B. Carpentieri, Efficient families of higher-order Caputo-type numerical schemes for solving fractional order differential equations, *Alex. Eng. J.*, **124** (2025), 337–361. https://doi.org/10.1016/j.aej.2025.02.111
36. N. Ali, M. Waseem, M. Safdar, A. Akgül, F. T. Tolasa, Iterative solutions for nonlinear equations via fractional derivatives: Adaptations and advances, *Appl. Math. Sci. Eng.*, **32** (2024), 2333816. https://doi.org/10.1080/27690911.2024.2333816
37. L. Cveticanin, *Strong nonlinear oscillators: Analytical solutions*, Springer Cham, 2018. https://doi.org/10.1007/978-3-319-58826-1
38. J. A. Conesa, *Chemical reactor design: Mathematical modeling and applications*, John Wiley & Sons, 2019. https://doi.org/10.1002/9783527823376
39. T. Kaczorek, K. Rogowski, *Fractional linear systems and electrical circuits*, Switzerland: Springer, 2015. https://doi.org/10.1007/978-3-319-11361-6

AIMS Press